Journal Title Here, 2023, 1–8
doi: DOI HERE
Paper

Changes in total charge on spike protein of SARS-CoV-2 in emerging lineages

Anže Božič[1] **and Rudolf Podgornik**[2,3,4]*

[1]Department of Theoretical Physics, Jožef Stefan Institute, 1000, Ljubljana, Slovenia, [2]School of Physical Sciences, University of Chinese Academy of Sciences, 100049, Beijing, China, [3]Kavli Institute for Theoretical Sciences, University of Chinese Academy of Sciences, 100049, Beijing, China and [4]Wenzhou Institute, University of Chinese Academy of Sciences, Wenzhou, 325001, Zhejiang, China

*Corresponding author. podgornikrudolf@ucas.ac.cn

Abstract

Motivation: Charged amino acid residues on the spike protein of severe acute respiratory syndrome coronavirus 2 (SARS-CoV-2) have been shown to influence its binding to different cell surface receptors, its non-specific electrostatic interactions with the environment, and its structural stability and conformation. It is therefore important to obtain a good understanding of amino acid mutations that affect the total charge on the spike protein which have arisen across different SARS-CoV-2 lineages during the course of the virus' evolution.
Results: We analyse the change in the number of ionizable amino acids and the corresponding total charge on the spike proteins of almost 2000 SARS-CoV-2 lineages that have emerged over the span of the pandemic. Our results show that the previously observed trend toward an increase in the positive charge on the spike protein of SARS-CoV-2 variants of concern has essentially stopped with the emergence of the early omicron variants. Furthermore, recently emerged lineages show a greater diversity in terms of their composition of ionizable amino acids. We also demonstrate that the patterns of change in the number of ionizable amino acids on the spike protein are characteristic of related lineages within the broader clade division of the SARS-CoV-2 phylogenetic tree. Due to the ubiquity of electrostatic interactions in the biological environment, our findings are relevant for a broad range of studies dealing with the structural stability of SARS-CoV-2 and its interactions with the environment.
Availability: The data underlying the article are available in the online Supplementary Material.

1. Introduction

The spike (S) protein of the severe acute respiratory syndrome coronavirus 2 (SARS-CoV-2) plays a role in target recognition, cellular entry, and endosomal escape of the virus (Huang et al., 2020). At the same time, the region in the viral genome that codes for the S protein is the one where most mutations tend to occur (Cavanagh, 2005; Harvey et al., 2021). Many of these mutations are intricately related to the changes in the structure of the S protein, thus influencing one or more of its functions (Mehra and Kepp, 2021). What is more, mutations on the S protein often lead to a change in its charge due to the ionizability of the corresponding amino acid (AA), and a series of recent studies has uncovered the tendency of these mutations to increase the amount of positive charge on the S protein (Pawłowski, 2021, 2022; Cotten and Phan, 2023; Božič and Podgornik, 2023).

Changes in the amount of charge on the receptor-binding domain (RBD) of the S protein have been explored in detail, with a number of studies showing that they can lead to an increased binding of the virus to the angiotensin-converting enzyme 2 (ACE2) receptor (Adhikari et al., 2022a,b; Nie et al., 2022; Gan et al., 2022; Kim et al., 2023; Barroso da Silva et al., 2022). However, the overall distribution of charged AAs on the S protein is not trivial: Although the stalk part is negatively charged, the top part of the spike molecule and RBD in particular remain predominantly positively charged for a broad range of pH values (Adamczyk et al., 2021; Kucherova et al., 2021). Surprisingly, the top of the spike also reveals an underlying core with a surface area that has a dense negative charge (Kucherova et al., 2021). Such a charge distribution promotes spike corona stability and enhances virion attachment to receptors and membrane surfaces, which are mostly negatively charged (Adamczyk et al., 2021). Nonuniform charge distribution of the S protein also plays an important role in the non-specific electrostatic interactions of the virus with other charged macromolecules and macromolecular substrates in its environment (Javidpour et al., 2021; Arbeitman et al., 2021; Nie et al., 2021, 2022; Zhang et al., 2023).

That charge on the S protein is an important factor in the evolution of SARS-CoV-2 is further supported by a very interesting finding by Pawłowski (2021), who observed a tendency of the mutations in the S protein of different variants of concern (VOCs) to increase the number of positively charged AA residues on it. Subsequent studies by Cotten and Phan (2023) and Božič and Podgornik (2023) confirmed this finding on larger datasets; however, they also provided the first indications that this steady progression toward ever larger positive charge on the S protein was coming to a halt with the newly emerging lineages. In order to resolve the question of whether the positive charge on the S protein of SARS-CoV-2 still has the capacity to increase as new lineages emerge and to obtain a better understanding of amino acid mutations that affect the total charge on the spike protein, we performed a study of the changes in the number of ionizable AAs on the S proteins of almost 2000 different SARS-CoV-2 lineages that have emerged between the start of the pandemic and August 2023. Our results show that not only has the increase in the amount of positive charge on the S protein stopped already with the early omicron variants, but that the pattern of AA changes and the resulting total charge have become more diverse with newly emerged lineages. Clustering the lineages based solely on the patterns of change in the number of ionizable AAs on their S proteins shows that these patterns are highly characteristic of different major clades and make it possible to distinguish between broad clusters of lineages.

2. Materials and Methods

2.1. Data collection

Our data collection follows the approach described in our previous study (Božič and Podgornik, 2023): We first collected a list of SARS-CoV-2 Pango lineages from `CoV-Lineages.org` lineage report (O'Toole et al., 2021) on September 8th 2023. These were then used as an input to download SARS-CoV-2 genomic and protein data from NCBI Virus database (Hatcher et al., 2017) on September 13th 2023. Accompanying annotations were used to extract the isolate collection dates, where we kept the earliest *full* record (i.e., year, month, and day) as the timepoint of lineage emergence for use in our analysis. Lineage divergence—the number of mutations in the *entire genome* relative to the root of the phylogenetic tree, i.e., the start of the outbreak—was obtained from the global SARS-CoV-2 data available on `Nextstrain.org` (Hadfield et al., 2018). We selected only those entries with a genome coverage of > 99 % and extracted their lineage divergence and the number of mutations. As the last step in the data selection, we retained only those Pango lineages whose downloaded fasta protein file was not empty. The total number of different SARS-CoV-2 lineages which passed this selection procedure and are included in our analysis is $N = 1965$. Since the number of S protein sequences included under each lineage varies, we consequently operate with average values taken over all sequences within a lineage; we denote these averages by $\overline{X}$.

2.2. Ionizable AAs and their charge

We use Biopython (Cock et al., 2009) to parse the S protein fasta files and count the number of ionizable AAs on the S proteins of different SARS-CoV-2 lineages. We consider six different ionizable AA types: aspartic (ASP) and glutamic acid (GLU), tyrosine (TYR), arginine (ARG), lysine (LYS), and histidine (HIS). We omit cysteine (CYS), since it has a thiol with a functional end group that is a very weak acid and is typically not considered to be an acid at all (Nap et al., 2014; Božič and Podgornik, 2017).

Table 1. Intrinsic pK_a values of AA functional groups in bulk dilute aqueous solutions. Values taken from Haynes (2014).

	ASP	GLU	TYR	ARG	LYS	HIS
pK_a	3.71	4.15	10.10	12.10	6.04	10.67

Three of the six AA types carry positive charge (ARG, LYS, and HIS), while the other three carry negative charge (ASP, GLU, and TYR). Using their bulk dissociation constants (Table 1) and the Henderson-Hasselbalch equation (Božič and Podgornik, 2017), we obtain the charge on them at a given pH:

$$q^{\pm} = \frac{\pm 1}{1 + \exp(\pm \ln 10(\mathrm{pH} - \mathrm{pK}_a))}. \tag{1}$$

From Eq. (1) and Table 1, one can for instance discern that HIS typically carries a relatively small fractional charge at physiological pH, while TYR starts to acquire charge only at very basic pH. The total charge on the S protein is then determined as the sum of contributions of individual ionizable AAs,

$$Q = \sum_{\mathrm{i} \in \mathrm{AA}} q_i^{\pm} \tag{2}$$

We are also interested in comparing the relative change in the number of ionizable AAs on the S proteins of different lineages to the wild-type (WT) version of the S protein. To this purpose, we introduce the measure $\overline{\delta}(\mathrm{AA})$,

$$\overline{\delta}(\mathrm{AA}) = \frac{\overline{N}(\mathrm{lineage})}{\overline{N}(\mathrm{WT\ B})} - 1, \tag{3}$$

which quantifies the relative change in the number of each individual ionizable AA type on the S protein of a given lineage compared to their number on the S protein of WT lineage B.

3. Results

3.1. Changes in the number of ionizable AAs on the S protein of different lineages

We first take a look at how the number of different ionizable AAs on the S protein has been changing during the course of the virus' evolution. Panel (a) of Fig. 1 shows the average number of ionizable AAs on the S protein as a function of the average lineage divergence, and thus also serves as a point of comparison to previous studies (Pawłowski, 2021, 2022; Cotten and Phan, 2023; Božič and Podgornik, 2023). Our dataset includes SARS-CoV-2 lineages from the first appearance of the virus at the end of the year 2019 all the way to the lineages that have emerged as late as August 2023, and Fig. 1a already indicates that among the recently emerged lineages there exist several subpopulations, each of which prefers a specific number of ionizable AAs. For instance, the number of GLU seems to take on roughly three separate values for different lineages with divergence $\gtrsim 70$. We can also observe that the pattern of increase in the number of positively charged AAs is more prominent for LYS and HIS residues, and less so for ARG. Moreover, the change in the number of a given AA type can vary anywhere between 5 (GLU) to 10 (LYS) residues among the different SARS-CoV-2 lineages.

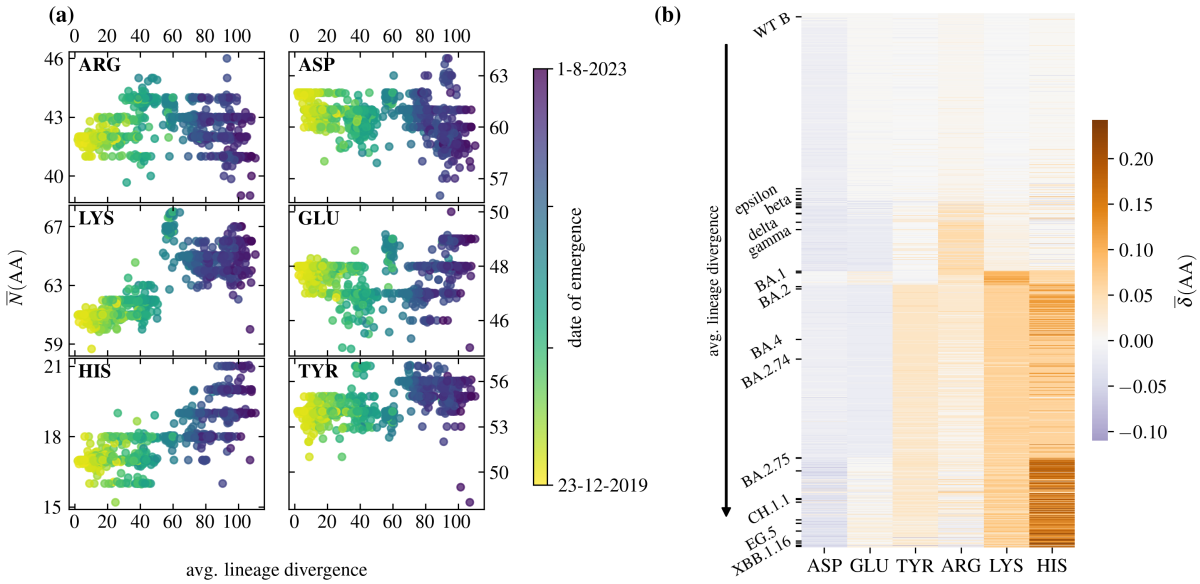

Fig. 1: **(a)** Evolution of the number of ionizable AAs on the S protein with the divergence of SARS-CoV-2 lineages. AAs in the first column (ARG, LYS, and HIS) take on a positive charge, while AAs in the second column (ASP, GLU, and TYR) take on a negative charge. Each point represents the average value over the sequences from a single lineage, its colour corresponding to the first recorded date of its emergence. **(b)** Heatmap of the relative change in the number of ionizable AAs compared to the WT (lineage B), arranged according to lineage divergence [Eq. (3)]. Ticks along the y-axis mark select VOCs and VBMs, also listed in Table 2.

Different patterns of change in the number of ionizable AAs on the S protein are made more visible in the heatmap in panel (b) of Fig. 1, which shows the relative change in the number of ionizable AAs for each of the 1965 lineages analyzed compared to the WT (lineage B) [Eq. (3)], arranged according to their average lineage divergence. Ticks on the y axis mark selected VOCs and variants being monitored (VBMs); these are listed in Table 2. While some changes seem prevalent across lineages, such as an increase in the number of LYS and TYR after the emergence of omicron, others—for instance, a significant increase in the number of HIS—do not occur regularly across lineages, even though they are more likely to be seen in the recently emerged ones.

3.2. Patterns of change in the number of ionizable AAs

In order to better understand the different patterns of change in the number of ionizable AAs in different lineages seen in Fig. 1, we perform k-means clustering on the profiles of relative changes in the AA numbers $\overline{\delta}$(AA) of all 1965 different lineages shown in Fig. 1b. In this way, we can observe which lineages are the most similar to each other in this respect. The optimal division of the lineages results in 7 clusters, and Fig. 2 shows their centroids—the mean relative changes in the number of ionizable AAs for all the lineages contained in the cluster. Assignment of each lineage in our dataset to one of the seven clusters is available in Supplementary Material.

The largest cluster (cluster index 1) shows almost no change in the number of ionizable AAs compared to the WT, while the cluster most similar to it, (2), already shows an increase in the number of ARG and a decrease in the number of ASP and GLU—pointing towards an overall increase in the total charge on the spike protein. This continues with cluster (3), where there is a significant increase in the number of LYS as well as an increase in the number of ARG and HIS. On the other hand, clusters (4) and (5), which are very similar to each other, show a decrease in the number of ASP and GLU, and an increase in the number of all other AA types. Finally, clusters (6) and (7) are the most distinct from all the others, one exhibiting a larger increase in LYS compared to HIS whereas the other exhibiting the opposite.

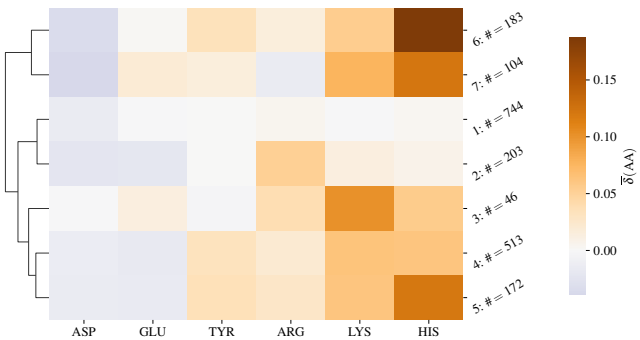

Fig. 2: Centroids of the 7 clusters obtained by k-means clustering of the relative changes in the number of ionizable AAs $\overline{\delta}$(AA) on the S proteins of 1965 SARS-CoV-2 lineages (Fig. 1b). Next to the numbered label of each cluster is the number of lineages that belong to it. The centroids are further hierarchically ordered as shown by the dendrogram on the left side.

Table 2. Table of main current and previous SARS-CoV-2 VOCs and VBMs. Listed are the average divergence of the lineage (the average number of mutations with respect to the root of the phylogenetic tree), the earliest known date of emergence of the lineage, the average total charge on the S protein $\overline{Q}$, and the cluster to which the lineage belongs to based on the changes in the number of ionizable AAs compared to WT. Full table of all 1965 analysed lineages is available in the Supplementary Material.

Lineage	Clade[1]	Avg. divergence[2]	Emergence[3]	$\overline{Q}$ $[e_0]$[4]	Cluster[5]
B	19B	4.36	2019-12-23	-5.29	1
B.1.427	epsilon	24.14	2020-10-14	-3.29	1
B.1.526	iota	25.22	2020-11-03	-1.77	1
P.2	zeta	25.81	2020-07-10	-2.29	1
B.1.351	beta	27.70	2020-10-09	-1.44	1
B.1.429	epsilon	28.09	2020-03-15	-3.28	1
B.1.525	eta	30.55	2020-12-15	-1.30	2
B.1.617.1	kappa	32.33	2021-02-08	-0.39	2
P.3	theta	33.03	2021-01-31	-0.11	1
C.37	lambda	33.79	2021-01-01	-4.17	1
B.1.621	mu	36.90	2021-04-20	-1.36	1
B.1.1.529	omicron	36.92	2020-10-20	-1.54	4
B.1.617.2	delta	38.55	2020-07-07	-0.54	2
P.1	gamma	39.58	2020-03-15	-3.38	1
BA.3	21M	55.38	2021-12-04	2.82	4
BA.1	21K	56.09	2020-12-22	1.90	3
BA.5	22B	67.71	2022-04-04	1.67	4
BA.2	21L	68.84	2020-09-02	1.85	5
BA.4	22A	73.21	2020-09-02	1.78	4
BA.2.74	21L	74.85	2022-05-28	1.00	5
XBB	22F	84.12	2022-09-20	0.27	7
BA.2.75	22D	84.19	2022-01-04	1.67	6
XBF	recombinant	89.95	2022-10-28	1.21	6
CH.1.1	23C	93.64	2022-09-29	1.15	6
XBK	recombinant	93.97	2022-11-07	1.22	6
XBB.1.5	23A	94.12	2021-11-22	0.29	7
XBB.1.9.1	23D	96.78	2022-12-29	0.08	7
XBB.2.3	23E	97.70	2022-12-21	0.93	7
EG.5	23F	99.62	2023-08-01	0.02	6
XBB.1.16	23B	103.56	2023-02-26	0.96	7
FL.1.5.1	23D	104.47	2023-05-20	-0.08	7
XBB.1.16.6	23B	107.13	2023-05-07	-2.28	1
DV.7.1	23C	108.00	2023-06-17	0.01	6

[1]Major variant or Nextclade (Aksamentov et al., 2021) clade designation.

[2]Average lineage divergence based on the number of mutations in the entire genome.

[3]Earliest full annotated date of lineage emergence.

[4]Average total charge on the S protein at pH = 7.

[5]Result of the k-means clustering into 7 clusters based on relative changes in the number of ionizable AAs.

3.3. Total charge on the S protein of different lineages

Next, we wish to estimate how the patterns of change in the number of ionizable AAs on the S protein translate into the amount of charge that the S protein carries. To this purpose, we determine the total charge on the S protein for each lineage in a simple fashion by using the Henderson-Hasselbalch equation with bulk pK_a values for each AA type (i.e., without taking into account the specific environment of each residue; see also Materials and Methods).

Figure 3 shows the average total charge on the S protein of 1965 different lineages as a function of their divergence for three different values of pH. Lineages are coloured according to the cluster they belong to (cf. Fig. 2). Despite lineage divergence not being a parameter of the clustering, the first three clusters, (1), (2), and (3), nicely follow the increase in the lineage divergence. The early lineages mostly fall under cluster (1) which shows fairly small changes in the number of ionizable AA compared to the WT (Fig. 2) and thus only a small increase in charge. The total charge nonetheless gradually increases with lineage divergence, and the spike proteins of lineages in cluster (2) already have a total charge around 0 at pH = 7. This cluster includes the early VOCs such as kappa and delta (Table 2 and Supplementary Material). Increasing the divergence still, the S proteins of lineages belonging to cluster (3) show quite an increase in charge, becoming overall positively charged at pH = 7; comparison with Fig. 2 indicates that this is likely mostly due to a large increase in the number of LYS. This

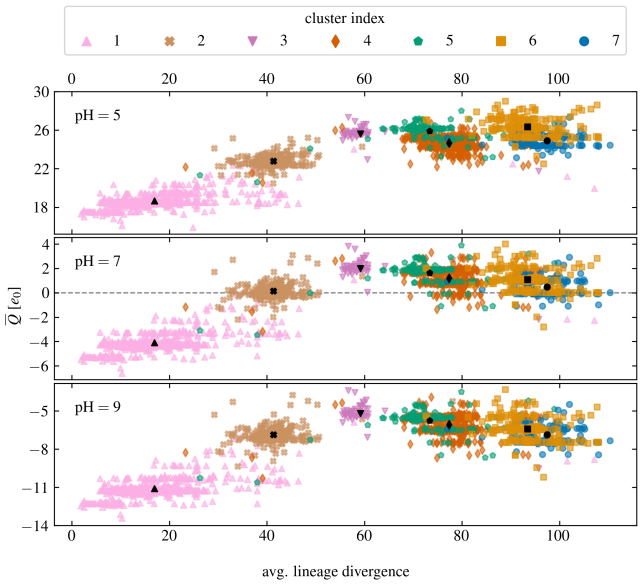

Fig. 3: Average total charge on the S proteins of 1965 different SARS-CoV-2 lineages at three different values of pH (pH = 5, 7, 9) as a function of average lineage divergence. Individual lineages are coloured according to the cluster of their relative change in the number of ionizable AAs to which they belong (cf. Fig. 2). Black symbols show the total charge according to the centroid of each cluster and are positioned at the mean divergence of the cluster.

cluster corresponds to the emergence of the early omicron lineages (Supplementary Material).

While the (average) changes in the number of ionizable AAs of clusters (4) and (5), which follow next, are different (Fig. 2), these changes do not lead to a significantly different amount of total charge on the S protein, albeit those belonging to cluster (5) have a slightly more positive charge. What is more, compared to the earlier cluster (3), the total charge on the S protein for the lineages in these two clusters is on average lower and shows a larger variability compared to the earlier cluster (3). Lastly, the (currently) most divergent clusters (6) and (7) are similar in this respect: While their profiles of the average change of ionizable AAs are the most distinct from among the 7 clusters (Fig. 2), the total charge on the S protein they lead to is lower than the peak reached with lineages in cluster (3). The total charge on the S proteins in these lineages is on average even lower than for the lineages in clusters (4) and (5). Similarly to these two clusters, the total charge on the S proteins of lineages in clusters (6) and (7) is also spread over a range of different values.

3.4. Placing the changes in charge on the S protein into the phylogenetic tree of SARS-CoV-2 lineages

We can also place each of the analysed lineages on the general phylogenetic tree of SARS-CoV-2 sequences to see whether their division into clusters based on the changes in the number of ionizable AAs on their S proteins corresponds to the phylogenetic division of their genomes. Figure 4 shows their placement on the phylogenetic tree generaged using Nextclade (Aksamentov et al., 2021), where each lineage is coloured according to the cluster it belongs to (Fig. 2). Interestingly, the clustering of the lineages—based *solely* on the changes in the number of ionizable AAs on the S proteins—corresponds extremely well to the broad division of lineages into different clades.

Cluster (1), with comparatively little change in the number of ionizable AAs compared to the WT, matches the earliest, least divergent clades of the phylogenetic tree, covering most VOCs up until omicron, as we have already noted before. Most of the lineages in cluster (2) belong to the major clade 21J and its descendants. Cluster (3) covers the clade 21K and indeed follows shortly after the emergence of omicron. Cluster (4) covers clades 22A, 22B, and 22E, while cluster (5) covers mainly the recombinant clade and a part of the clade 21L. Cluster (6) includes clades 22D and 23C, while cluster (7) covers most other recently emerged clades, including 22F, 23A, 23B, 23D, 23E, and 23F.

Figures 3 and 4 together make it clear that while the total charge on the S protein of SARS-CoV-2 gradually became positive with the emergence of new lineages, it has reached a peak with the early omicron variants (cluster (3)). At neutral and basic values of pH, more divergent lineages (clusters (4)–(7)) retain the overall increase in the amount of positive charge on the S protein, but this charge has not only stopped increasing but also decreased slightly on average, as can be seen from the total charge according to the centroids of the clusters (black symbols). In contrast, the mutations in the ionizable AAs on the S proteins of recently emerged lineages show that these mutations retain the increase in positive charge at acidic values of pH, even increasing it slightly further.

There are also some notable lineages which stand out from the clusters in Fig. 4. In particular, some lineages in the branch belonging to cluster (7) have a charge profile of the S protein more similar to those in cluster (6), while a few of them even have the charge profile belonging to the initial cluster (1). A prominent example of the latter is the lineage XBB.1.16.6, whose charge on the S protein seems to have reverted to that of the early lineages, as can be also discerned from Table 2.

4. Discussion and conclusions

By studying the changes in the number of ionizable AAs on the S protein of 1965 different SARS-CoV-2 lineages which have emerged between the start of the pandemic and August 2023 (Fig. 1), we have shown that these have initially led to a significant increase in the positive charge on the S protein with the emergence of early omicron variants, but that this increase has stopped and even reverted slightly with newly emerged lineages (Fig. 3). Our results also indicate that the recent changes in the ionizable AAs lead to S proteins whose charge is slightly reduced at neutral and basic pH compared to earliest omicron variants, while retains high values at acidic pH (Fig. 3). Given that is has been previously shown that the stability and activity of SARS-CoV-2 are significantly suppressed at very acidic and very basic pH, pH < 5 and pH > 9 (Chan et al., 2020), it would be interesting to explore the functional importance of mutations which retain high positive charge of the S protein at acidic pH.

We have furthermore extracted 7 distinct patterns of relative change in the number of different ionizable AA types (Fig. 2), which not only follow along with the divergence of the lineages (Fig. 3) but also cover the broad division into major clades of the SARS-CoV-2 phylogenetic tree (Fig. 4). The latter observation is in line with previous studies which have demonstrated the possibility that VOCs could be identified from the sequence of the S protein alone,

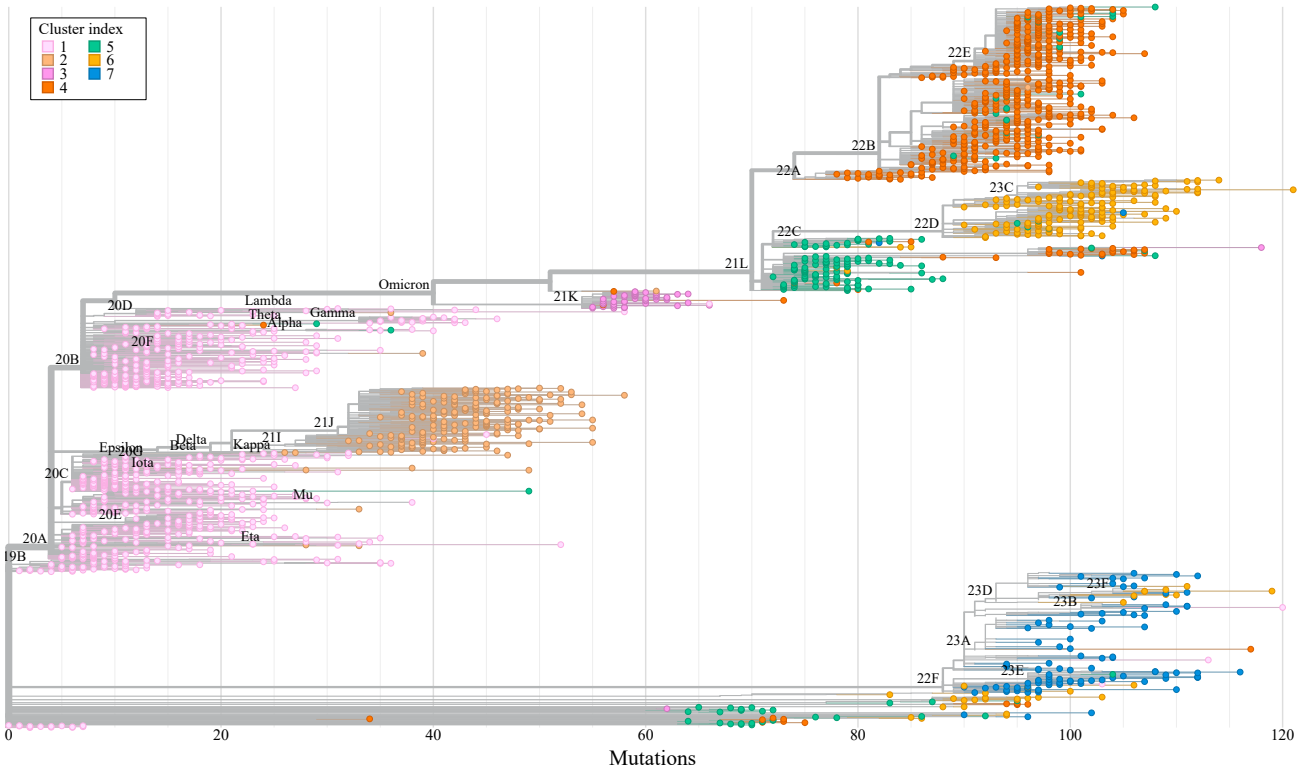

Fig. 4: Placement of the 1965 SARS-CoV-2 lineages analysed in this work on the phylogenetic tree of all SARS-CoV-2 lineages as provided by Nextclade (Aksamentov et al., 2021). Only a single sequence of each analysed lineage is shown for clarity, and the tree is annotated with the major Nextstrain clades (Hadfield et al., 2018). Individual lineages are coloured according to the cluster of their relative change in the number of ionizable AAs to which they belong (cf. Fig. 2).

which would make lineage assignment relatively easier compared to the use of complete genome sequences (O'Toole et al., 2022).

The total charge on the S protein that we determine here should be seen only as a proxy. While the values correspond to those obtained in studies using a similar approach (Pawłowski, 2021, 2022; Cotten and Phan, 2023), studies using more detailed structural models that took into account local changes in the dissociation constants in general obtained higher values, even though these still vary among different studies (Adamczyk et al., 2021; Kim et al., 2023). However, inclusion of such details would require knowing the correct structure of the S protein for each and every lineage included in our study (Mehra and Kepp, 2021; Casalino et al., 2020), which is impossible to obtain, and to truly determine the correct charge on the S protein, one would have to resort to simulations based on density functional theory (Ching et al., 2023), which is computationally prohibitive for such a large dataset. Despite using a very simple model, we are nonetheless able to observe the trends seen in studies using more detailed models (Kim et al., 2023; Barroso da Silva et al., 2022); thus, while the values of charge on the S protein we determine are certainly not exact, the patterns we see should translate even to studies using more accurate models for the charge on the AA residues.

The results of our work are relevant for a broad range of studies involving SARS-CoV-2: The relevance of the changes in the number of ionizable AAs on the S protein goes beyond those which occur in the RBD of the protein and which have direct implications for its binding to the ACE2 receptor. Some of these mutations can play a role in (de)stabilizing or altering the structure of the S protein in either closed or open states (Warwicker, 2021; Boer et al., 2022), while mutations occurring in other parts of the S protein can be a consequence of adaptation to more general electrostatic interactions with the environment of the virus, for instance with lipid rafts in cellular membranes (Matveeva et al., 2023).

Data availability

Data presented in this work are available in the online Supplementary Material.

Competing interests

No competing interest is declared.

Author contributions statement

R.P. conceived the study and A.B. performed the analysis and analysed the results. A.B. and R.P. wrote and reviewed the manuscript.

Acknowledgments

We thank Domen Vaupotič for help with preparing Figure 4.

Funding information

This work was supported by Slovenian Research Agency (ARRS) [P1-0055 to A.B.] and the National Natural Science Foundation of China (NSFC) [Key Project 12034019 to R.P.].

References

Z. Adamczyk, P. Batys, and J. Barbasz. SARS-CoV-2 virion physicochemical characteristics pertinent to abiotic substrate attachment. *Curr. Op. Colloid Interface Sci.*, 55:101466, 2021.

P. Adhikari, B. Jawad, R. Podgornik, and W.-Y. Ching. Mutations of omicron variant at the interface of the receptor domain motif and human angiotensin-converting enzyme-2. *Int. J. Mol. Sci.*, 23:2870, 2022a.

P. Adhikari, B. Jawad, R. Podgornik, and W.-Y. Ching. Quantum chemical computation of omicron mutations near cleavage sites of the spike protein. *Microorganisms*, 10:1999, Oct. 2022b.

I. Aksamentov, C. Roemer, E. B. Hodcroft, and R. A. Neher. Nextclade: clade assignment, mutation calling and quality control for viral genomes. *J. Open Source Softw.*, 6:3773, 2021.

C. R. Arbeitman, P. Rojas, P. Ojeda-May, and M. E. Garcia. The SARS-CoV-2 spike protein is vulnerable to moderate electric fields. *Nat. Commun.*, 12:5407, 2021.

F. L. Barroso da Silva, C. C. Giron, and A. Laaksonen. Electrostatic features for the receptor binding domain of SARS-COV-2 wildtype and its variants. compass to the severity of the future variants with the charge-rule. *J. Phys. Chem. B*, 126:6835–6852, 2022.

J. C. Boer, Q. Pan, J. K. Holien, T.-B. Nguyen, D. B. Ascher, and M. Plebanski. A bias of asparagine to lysine mutations in SARS-CoV-2 outside the receptor binding domain affects protein flexibility. *Front. Immunol.*, page 954435, 2022.

A. Božič and R. Podgornik. pH dependence of charge multipole moments in proteins. *Biophys. J.*, 113:1454–1465, 2017.

A. Božič and R. Podgornik. Evolutionary changes in the number of dissociable amino acids on spike proteins and nucleoproteins of SARS-CoV-2 variants. *Virus Evol.*, 9:vead040, 2023.

L. Casalino, Z. Gaieb, J. A. Goldsmith, C. K. Hjorth, A. C. Dommer, A. M. Harbison, C. A. Fogarty, E. P. Barros, B. C. Taylor, J. S. McLellan, et al. Beyond shielding: the roles of glycans in the SARS-CoV-2 spike protein. *ACS Cent. Sci.*, 6: 1722–1734, 2020.

D. Cavanagh. Coronaviridae: a review of coronaviruses and toroviruses. In A. Schmidt, M. Wolff, and O. Weber, editors, *Coronaviruses with special emphasis on first insights concerning SARS*, pages 1–54. Birkhäuser Verlag, Basel, 2005.

K. H. Chan, S. Sridhar, R. R. Zhang, H. Chu, A.-F. Fung, G. Chan, J.-W. Chan, K.-W. To, I.-N. Hung, V.-C. Cheng, et al. Factors affecting stability and infectivity of SARS-CoV-2. *J. Hosp. Infect.*, 106:226–231, 2020.

W.-Y. Ching, P. Adhikari, B. Jawad, and R. Podgornik. Towards quantum-chemical level calculations of SARS-CoV-2 spike protein variants of concern by first principles density functional theory. *Biomedicines*, 11:517, Feb. 2023.

P. J. Cock, T. Antao, J. T. Chang, B. A. Chapman, C. J. Cox, A. Dalke, I. Friedberg, T. Hamelryck, F. Kauff, B. Wilczynski, et al. Biopython: freely available Python tools for computational molecular biology and bioinformatics. *Bioinformatics*, 25:1422, 2009.

M. Cotten and M. V. Phan. Evolution of increased positive charge on the SARS-CoV-2 spike protein may be adaptation to human transmission. *iScience*, 26:106230, 2023.

H. H. Gan, J. Zinno, F. Piano, and K. C. Gunsalus. Omicron spike protein has a positive electrostatic surface that promotes ACE2 recognition and antibody escape. *Front. Virol.*, 2, 2022.

J. Hadfield, C. Megill, S. M. Bell, J. Huddleston, B. Potter, C. Callender, P. Sagulenko, T. Bedford, and R. A. Neher. Nextstrain: real-time tracking of pathogen evolution. *Bioinform.*, 34:4121–4123, 2018.

W. T. Harvey, A. M. Carabelli, B. Jackson, R. K. Gupta, E. C. Thomson, E. M. Harrison, C. Ludden, R. Reeve, A. Rambaut, C.-. G. U. C.-U. Consortium, et al. SARS-CoV-2 variants, spike mutations and immune escape. *Nat. Rev. Microbiol.*, 19:409–424, 2021.

E. L. Hatcher, S. A. Zhdanov, Y. Bao, O. Blinkova, E. P. Nawrocki, Y. Ostapchuck, A. A. Schäffer, and J. R. Brister. Virus variation resource—improved response to emergent viral outbreaks. *Nucleic Acids Res.*, 45(D1):D482–D490, 2017.

W. M. Haynes. *CRC handbook of chemistry and physics*. CRC press, 2014.

Y. Huang, C. Yang, X.-f. Xu, W. Xu, and S.-w. Liu. Structural and functional properties of SARS-CoV-2 spike protein: potential antivirus drug development for COVID-19. *Acta Pharmacol. Sin.*, 41:1141–1149, 2020.

L. Javidpour, A. Božič, A. Naji, and R. Podgornik. Electrostatic interactions between the SARS-CoV-2 virus and a charged electret fibre. *Soft Matter*, 17:4296–4303, 2021.

S. H. Kim, F. L. Kearns, M. A. Rosenfeld, L. Votapka, L. Casalino, M. Papanikolas, R. E. Amaro, and R. Freeman. SARS-CoV-2 evolved variants optimize binding to cellular glycocalyx. *Cell Rep. Phys. Sci.*, 4, 2023.

A. Kucherova, S. Strango, S. Sukenik, and M. Theillard. Computational modeling of protein conformational changes—application to the opening SARS-CoV-2 spike. *J. Comp. Phys.*, 444:110591, 2021.

M. Matveeva, M. Lefebvre, H. Chahinian, N. Yahi, and J. Fantini. Host membranes as drivers of virus evolution. *Viruses*, 15:1854, 2023.

R. Mehra and K. P. Kepp. Structure and mutations of SARS-CoV-2 spike protein: a focused overview. *ACS Infect. Dis.*, 8:29–58, 2021.

R. J. Nap, A. Božič, I. Szleifer, and R. Podgornik. The role of solution conditions in the bacteriophage PP7 capsid charge regulation. *Biophys. J.*, 107:1970–1979, 2014.

C. Nie, P. Pouyan, D. Lauster, J. Trimpert, Y. Kerkhoff, G. P. Szekeres, M. Wallert, S. Block, A. K. Sahoo, J. Dernedde, et al. Polysulfates block SARS-CoV-2 uptake through electrostatic interactions. *Angew. Chem. Int. Ed.*, 60:15870–15878, 2021.

C. Nie, A. K. Sahoo, R. R. Netz, A. Herrmann, M. Ballauff, and R. Haag. Charge matters: Mutations in omicron variant favor binding to cells. *ChemBioChem*, 23:e202100681, 2022.

Á. O'Toole, V. Hill, O. G. Pybus, A. Watts, I. I. Bogoch, K. Khan, J. P. Messina, T. COVID, B.-U. C. G. Network, H. Tegally, et al. Tracking the international spread of SARS-CoV-2 lineages B.1.1.7 and B.1.351/501Y-V2 with grinch. *Wellcome Open Res.*, 6, 2021.

Á. O'Toole, O. G. Pybus, M. E. Abram, E. J. Kelly, and A. Rambaut. Pango lineage designation and assignment using SARS-CoV-2 spike gene nucleotide sequences. *BMC Genom.*, 23:1–13, 2022.

P. Pawłowski. SARS-CoV-2 variant omicron (B. 1.1. 529) is in a rising trend of mutations increasing the positive electric charge in crucial regions of the spike protein S. *Acta Biochim. Pol.*, 69: 263–264, 2022.

P. H. Pawłowski. Additional positive electric residues in the crucial spike glycoprotein S regions of the new SARS-CoV-2 variants. *Infect. Drug Resist.*, 14:5099–5105, 2021.

J. Warwicker. A model for ph coupling of the SARS-CoV-2 spike protein open/closed equilibrium. *Brief. Bioinformatics*, 22: 1499–1507, 2021.

S. Zhang, N. Wang, Q. Zhang, R. Guan, Z. Qu, L. Sun, and J. Li. The rise of electroactive materials in face masks for preventing virus infections. *ACS Appl. Mater. Interfaces*, 2023.